of the eelgrass *Zostera marina* (*59*) in the North Atlantic and of the mass mortality of corals in the eastern Pacific related to the El Niño (*9, 54, 55*).

Note added in proof: Mass mortality reached Tobago in mid-February (*60*).

H. A. LESSIOS
D. R. ROBERTSON
J. D. CUBIT
Smithsonian Tropical Research Institute, Balboa, Panama

References and Notes

1. J. E. Randall, R. E. Schroeder, W. A. Stark, *Caribb. J. Sci.* **4**, 421 (1964).
2. P. W. Sammarco, *J. Exp. Mar. Biol. Ecol.* **45**, 245 (1980); *ibid.* **61**, 31 (1982); *ibid.* **65**, 83 (1982).
3. C. W. Stearn and T. P. Scoffin, *Proc. Third Int. Coral Reef Symp.* **2**, 471 (1977).
4. R. P. M. Bak and G. van Eys, *Oecologia (Berlin)* **20**, 111 (1975).
5. R. C. Carpenter, *J. Mar. Res.* **39**, 749 (1981).
6. A. H. Williams, *Ecology* **62**, 1107 (1981).
7. J. E. Randall, *ibid.* **42**, 812 (1961); A. H. Williams, *Oecologia (Berlin)* **38**, 223 (1979); *Am. Nat.* **116**, 138 (1980); P. W. Sammarco and A. H. Williams, *Mar. Ecol. Prog. Ser.* **8**, 53 (1982).
8. J. C. Ogden, R. A. Brown, N. Salesky, *Science* **182**, 715 (1973).
9. H. A. Lessios, P. W. Glynn, D. R. Robertson, *ibid.* **222**, 715 (1983).
10. H. A. Lessios *et al.*, *Coral Reefs*, in press.
11. T. P. Hughes, B. D. Keller, J. B. C. Jackson, M. J. Boyle, *Bull. Mar. Sci.*, in press.
12. 41. R. P. M. Bak, M. J. E. Carpay, E. D. de Ruyter van Steveninck, *Mar. Ecol. Prog. Ser.* **17**, 105 (1984).
13. We sent questionnaires to the institutions listed in the Unesco directory of Caribbean marine laboratories [*Directory of Caribbean Marine Research Centers* (United Nations Environment Programme and Intergovernmental Oceanographic Commission, Geneva, 1980)] and to diving resorts and tour boat operators advertising in diving magazines. We asked if mass mortality of *D. antillarum* had been observed in their areas, if the symptoms exhibited by affected animals conformed to those observed in Panama, when the mortality was first noted, and when populations were last seen to be healthy. We received 86 replies from 25 countries. We subsequently followed the situation in areas initially reported to be free of mortality through further communication with local marine laboratories. Scientists visiting various areas of the Caribbean also responded to our published request for information (*9*). We took information from scientists at face value. Questionnaires answered by divers were often inconsistent as to the timing of appearance of mortality; in such cases we relied on the information provided by scientists for the same area and considered questionnaires from divers as corroborating that mortality had occurred in their areas. Only for two countries, Mexico and Haiti, was there no information from scientists, forcing us to rely entirely on the reports of divers.
14. J. Burgett (Smithsonian Tropical Research Institute, Balboa, Panama), personal communication.
15. A. A. Acero, S. Zea, J. Gallo (Instituto de Investigaciones Marinas, Santa Marta, Colombia), personal communications.
16. M. Murillo (Universidad de Costa Rica, San José), personal communication.
17. G. Wust, *Stratification and Circulation in the Antillean-Caribbean Basins* (Columbia Univ. Press, New York, 1964), pp. 66–67.
18. T. H. Kinder, *Bull. Mar. Sci.* **33**, 239 (1983).
19. K. S. Gomez and J. Parsons (Cayman Department of Agriculture, Lands, and Natural Resources, Cayman Islands), personal communication.
20. A. Gordon, *J. Geophys. Res.* **72**, 6207 (1967).
21. R. L. Molinari, M. Spillane, I. Brooks, D. Atwood, C. Duckett, *ibid.* **86**, 6537 (1981).
22. J. Woodley (Discovery Bay Marine Laboratory, Jamaica), personal communication.
23. C. J. Grant and J. R. Wyatt, *Bull. Mar. Sci.* **30**, 613 (1980).
24. L. Wodarski, personal communication.
25. G. Bevier, personal communication; the mortality was definitely absent in late June [K. Ruetzler (Smithsonian Institution, Washington, D.C.) and N. Engstrom (Northern Illinois University, DeKalb), personal communications].
26. J. T. Brucks, *Bull. Mar. Sci.* **21**, 455 (1971).
27. J. C. Halas (Department of Natural Resources, Key Largo, Fla.), personal communication.
28. B. Causey (Department of Natural Resources, Looe Key, Fla.), personal communication.
29. C. R. Kruger (U.S. Army Corps of Engineers, Big Pine Key, Fla.), personal communication; J. Tilmant (National Park Service, Homestead, Fla.), personal communication.
30. W. Düing and D. Johnson, *Science* **173**, 428 (1971); P. P. Niiler and W. S. Richardson, *J. Mar. Res.* **31**, 144 (1973); T. N. Lee, *Deep-Sea Res.* **22**, 753 (1975); W. Düing, *J. Mar. Res.* **33**, 53 (1975); I. Brooks and P. Niiler, *ibid.* **35**, 163 (1977).
31. G. B. Smith (Food and Agriculture Organization, United Nations, Nassau), personal communication; B. Blonder (Forfar Field Station, Andros), personal communication.
32. R. A. Cameron (University of Puerto Rico, Mayaguéz), personal communication.
33. J. Brown, personal communication.
34. S. Jakowska and I. Bonnelly (Centro de Investigacion de Biologia Marina, Santo Domingo), personal communication.
35. A. M. Baskin, personal communication.
36. B. E. Luckhurst (Division of Fisheries, Bermuda), personal communication; T. G. Rand (Bermuda Aquarium, Natural History Museum and Zoo), personal communication.
37. P. Wiebe, *Oceanus* **193**, 69 (1976).
38. U.S. Navy and National Weather Service–National Earth Satellite Service data, Woods Hole Oceanographic Institution, Woods Hole, Mass.
39. W. Hunte (Bellairs Research Institute, Barbados), personal communication.
40. I. Emilsson, *Geofiz. Int.* **11**, 139 (1971).
41. D. Meyer (University of Cincinnati), personal communication.
42. R. Laughlin (Fundacion Cientifica Los Roques, Caracas), personal communication.
43. D. Ramsaroop (Institute of Marine Affairs, Trinidad and Tobago), personal communication.
44. A. Smith (Seamoss Mariculture Project, St. Lucia, West Indies), personal communication; P. N. Pietruszka, personal communication.
45. C. Bouchon (Centre Universitaire Antilles-Guyane, Guadeloupe), personal communication.
46. F. Geraldes, H. Pugibet, M. Ramirez (Museo Nacional de Historia Natural, Santo Domingo), personal communication.
47. R. Boulon, Jr. (Division of Fish and Wildlife, St. Thomas, U.S. Virgin Islands), personal communication.
48. L. Walters (Ministry of Natural Resources and Environment, Tortola, British Virgin Islands), personal communication; R. C. Murphy (Cousteau Society, Los Angeles, Calif.), personal communication.
49. R. Wilkins (Ministry of Agriculture, Lands, Housing, Labour and Tourism, St. Kitts, British West Indies), personal communication.
50. J. Ogden (West Indies Laboratory, St. Croix, U.S. Virgin Islands), personal communication.
51. R. J. Miller and A. G. Colodey, *Mar. Biol.* **73**, 263 (1983); R. E. Scheibling and R. L. Stephenson, *ibid.* **78**, 153 (1984).
52. *Echinometra viridis, E. lucunter, Lytechinus variegatus, L. williamsi, Tripneustes ventricosus*, and *Eucidaris tribuloides*.
53. P. W. Glynn, *Environ. Conserv.*, in press.
54. H. A. Lessios, *Evolution* **35**, 618 (1981).
55. P. W. Glynn, *Environ. Conserv.*, **10**, 149 (1983).
56. F. G. W. Smith, *Ecology* **22**, 415 (1941).
57. J. S. Pearse, D. P. Costa, M. B. Yellin, C. R. Agegian, *Fish. Bull.* **75**, 645 (1977).
58. M. L. Dungan, T. E. Miller, D. A. Thomson, *Science* **216**, 989 (1982).
59. E. Rasmussen, in *Seagrass Ecosystems*, C. P. McRoy and C. Helfferich, Eds. (Dekker, New York, 1977), p. 1.
60. R. Laydoo (Institute of Marine Affairs, Trinidad and Tobago), personal communication.
61. United States Naval Oceanographic Office and National Oceanic and Atmospheric Administration, *Pilot Chart of the North Atlantic Ocean* (Defense Mapping Agency Hydrographic–Topographic Center, Washington, D.C., 1982).
62. We thank J. Burgett, who was the first person to report the *Diadema* mortality; J. Halas, R. Causey, and C. Curtis, who made work in Florida possible; R. Boulon, who similarly helped in St. Thomas; and all the people referenced above, who provided information about the status of *Diadema* populations in their areas. R. Schmidt and F. Grassle provided unpublished oceanographic data. P. W. Glynn, T. H. Kinder, R. L. Molinari, F. A. Neva, and R. E. Scheibling commented on the manuscript. This research was supported by general research funds from the Smithsonian Tropical Research Institute and grants from the Scholarly Studies and the Environmental Sciences programs of the Smithsonian Institution.

10 February 1984; accepted 26 March 1984

The Jovian Nebula: A Post-Voyager Perspective

Abstract. *Voyager 1 carried a diverse collection of magnetospheric probes through the inner Jovian magnetosphere in March 1979. The ensuing data analysis and theoretical investigation provided a comprehensive description of the Jovian nebula, a luminous torus populated with newly released heavy ions drawn from Io's surface. Recent refinements in Earth-based imaging instrumentation are used to extend the Voyager in situ picture in temporal and spatial coverage. An analysis of [SIII] and [SII] optical emissions observed during the Jovian apparitions of 1981 through 1983 reveals three distinct torus components. Regularities have been identified in the ion partitioning and ion densities in the hot outer and inner tori, sharply defined radial structure is found in the plasma near Io, and the relative permanence of the cool inner torus is inferred. An extended cloud of neutral material is required as a source of fresh ions in the nebula.*

The Io torus was extensively probed during the Voyager 1 flyby in March 1979 with a trajectory that penetrated the Jovian magnetosphere to distances within the orbit of Io (*1*). With Io as a source of heavy ions, Jovian rotation as an energy source, and Jupiter's magnetic field as a confinement mechanism, the Io torus nevertheless exhibits many characteristics typical of ionized gas found in planetary nebulae and thus the "Jovian nebula" is also accessible to Earth-based astronomy. This is the first astronomical nebula to be studied both by the methods of classical astronomy and by in situ measurements. Earth-based astronomy provides coverage of the entire nebula over an extended period of time, bridging the gaps between infrequent spacecraft visits to Jupiter.

The Jovian magnetic field imposes a well-defined geometry upon the Iogenic plasma distribution. Jupiter presents a nearly undistorted dipole magnetic field

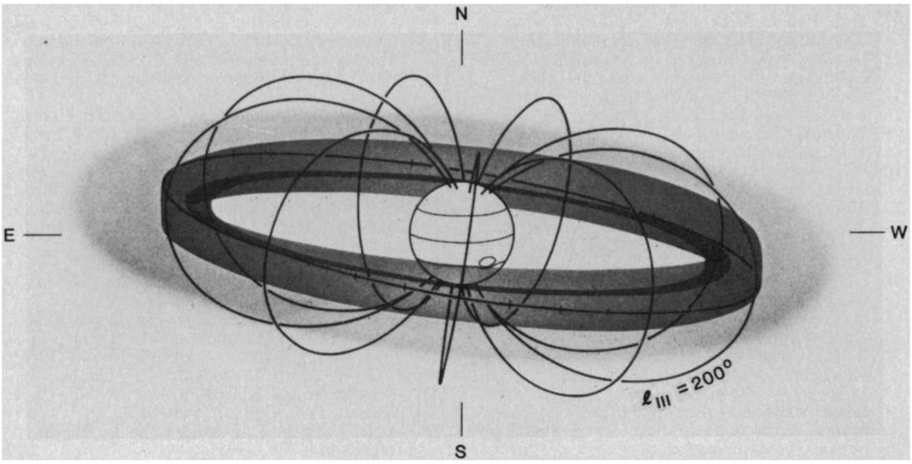

Fig. 1. Sketch of the torus structure within the Jovian nebula. Three concentric components are depicted: a diffuse hot outer torus outside Io's orbit, a narrow ribbon-like hot inner torus closely confined inside Io's orbit, and a relatively flat and isolated cool inner torus. The torus structure is tilted 7° from the rotational equator, so that it appears at a variety of projected angles during each Jovian rotation. The false-color images in Fig. 3 show the ansa of this structure as it is seen projected against the plane of the sky.

in the vicinity of Io's orbit, which is tilted 10.8° from the rotational axis and offset from the planet center by about 0.1 Jovian radius ($R_{♃}$) (2). Within this dipole field, ions are forced to corotate with the planet and gyrate tightly about the lines of force with periods on the order of seconds. Particle mirroring along the field lines is dominated by corotational centrifugal forces, with bounce periods of about 6 hours. Ions are driven by centrifugal forces toward positions on the field lines most distant from the rotational axis, thus defining the equilibrium "centrifugal confinement equator." This equator has 2/3 the tilt of the Jovian dipole or about 7° (3). The corotating magnetic field overtakes Io at a rate of 57 km sec^{-1}, about twice per day, and as a result ions supplied by Io are effectively distributed into a toroidal geometry.

The physical mechanism by which Io supplies material to the Jovian magnetosphere is not well understood, but it almost certainly involves the sputtering of material from the satellite surface or its tenuous atmosphere by heavy magnetospheric ions. These heavy ions originated as sputtered neutrals from Io; hence a feedback mechanism is at work, and we anticipate that the system is capable of significant temporal change. The composition of sputtered material is linked to the surface geology and atmosphere of Io, which are subject to fluctuations in volcanic activity and diurnal cycles in solar heating. The tilt of the Jovian magnetic dipole leads to periodic variations in Io's magnetic coordinates and may impose longitudinal structure in the torus. The diverse processes that drive time variations in other observed magnetospheric phenomena (notably the Jovian aurora and Io-modulated decametric radio storms) may ultimately affect the Jovian plasma torus as well.

In addition to potential time changes, the Jovian nebula has important radial and longitudinal structure in plasma density and temperature (4). As a result, we must anticipate potential difficulties in the synthesis of independent experimental measurements of diverse torus phenomena at various epochs over periods of years. Voyager 1 provided a comprehensive in situ "snapshot" focused on a limited volume of the Io torus during the Jovian encounter in March 1979; hence consistency is expected within the Voyager data set. It is clear that an optimum strategy for Earth-based observations requires a self-supporting collection of simultaneous measurements.

The recent availability of the silicon charged coupled device (CCD) detector has made it possible to collect photometric images of a number of visible and near-infrared [SII] and [SIII] emission lines (from S^+ and S^{2+} ions, respectively) excited by collisions with thermal electrons (energy ≤ 5 eV). These in turn provide a map of ion and electron densities and characteristic temperatures of the plasma (5). Hence a self-supported description of the nebula can be established on a given observing date and variations can be charted over larger time intervals, providing a framework for understanding the diverse and sometimes apparently contradictory results reported over the years since its discovery in 1975 (4).

The Voyager in situ snapshot led to a description of the Jovian nebula in terms of two components, a hot torus centered at Io's orbit and a concentric cool torus inside its orbit (6). In this analysis I illustrate the necessity of further resolving the Voyager two-component picture into three distinct regions, based on CCD imaging with a narrow-band coronagraphic instrument at the Las Campanas 2.5-m telescope during the Jovian apparitions in 1981 through 1983. These components are schematically shown in Fig. 1 superimposed on a sketch of the planet and its magnetic lines.

The data are monochromatic images taken in sequence among the diagnostic spectral lines emitted by the torus ions. Individual frames are corrected for instrumental brightness irregularities and spectral information encoded in the field of view, and residual scattered Jovian continuum radiation is subtracted. The resulting frames support 10 percent photometry (absolute intensities are known to 10 percent), and the background subtraction is accurate to within about 10 rayleighs in individual 0.75 arc-second pixels. A radial trace through a representative sequence of frames is shown in Fig. 2a. This set consists of three consecutive frames among 24 obtained on the evening of 4 May 1983 as the nebula rotated through the instrument field of view west of Jupiter. The corresponding image is represented in false color in Fig. 3b. Inspection of the extensive data set has amply demonstrated that the torus properties vary smoothly with longitude and that comparisons between successive frames provide reliable line intensity ratios for analysis. The wavelengths and system III (1965) longitudes ℓ_{III} at the ansa of the torus were, respectively, [SIII] 9531 Å at 32°, [SII] 6731 Å at 39°, and [SII] 6716 Å at 46°. Because of the 7° tilt and the −3° Jovicentric declination of Earth, a nearly edge-on projection of the torus is seen. These three frames are discussed specifically in the following paragraphs, but reference is made to general tendencies that are apparent in the full set of images.

A model is used to unfold the three-dimensional structure from the two-dimensional projections apparent in the images. A model-integrated brightness

$$4\pi J' = 10^{-6} \int E \, ds$$

(where J' is in rayleighs) along the line of sight s is computed after setting up a trial torus structure and the viewing geometry appropriate for a given data frame. The emission rate E (in photons per cubic centimeter per second) from each point in the torus is separated into simple functions of radial distance $R(r)$ from Jupiter and latitude separation $L(\lambda)$ along field lines from the centrifugal confinement equator:

$$E(r,\lambda) = E_0 R(r) L(\lambda)$$

Both coordinates are measured in R_J units. The radial functions $R(r)$ are discussed in following sections. The latitude separations

$$L(\lambda) = [n_e(\lambda)/n_e(0)] \exp\text{-}(\lambda^2/H^2)$$

define ion temperatures T_I (in electron volts) in terms of sulfur ion–density scale heights (*7*):

$$H = 0.112\ T_I^{1/2}\ R_J$$

The electron densities n_e are built up in terms of the total ion population, and a multicomponent torus structure is assembled and refined as a sum of individual model components. This procedure has proven sufficient to produce an excellent match to the observations in each frame, and characteristic three-dimensional radial and latitudinal structure may be extracted in terms of simple functions.

The extracted emission rates $E(r,\lambda)$ determine the product of electron and ion densities ($n_e n_I$) at each point in space in terms of theoretical electron collision cross sections and radiative lifetimes (*8*). An electron temperature is required, which is taken to be 5 eV in the outer torus on the basis of the observed [SIII] 6312/9531 ratio, approximately equal to 0.13 throughout the region. This is consistent with post-1979 Voyager extreme ultraviolet spectra in the hot outer torus (*9*). An electron temperature of 2 eV was used in the cool inner torus. The resulting radial structure in $n_e n_I$ at the centrifugal equator is illustrated in the curves in Fig. 2b. An equatorial n_e distribution is inferred from the model 6716/6731 ratios and is shown in Fig. 2c. The distributions in n_e and $n_e n_I$ together determine the ion densities.

Hot outer torus. The plasma exterior to Io's orbital path, extending from about 5.9 to at least 7 R_J, is characterized by a superposition of S^+ and S^{2+} ions at a common temperature. Values of T_I inferred from the modeled $L(\lambda)$ are consistently between 30 and 50 eV in images from the 1981 to 1983 apparitions. Similar T_I values were obtained in the outer torus with the Voyager 1 charged particle experiment (*6*). The radial decrease in both S^+ and S^{2+} n_I values is well represented by

$$R(r) = \exp - [(r - 5.9)/K]$$

between 6 and 7 R_J with $K = 1.2\ R_J$. As a consequence, the ion partitioning between these two species remains fixed, with a number ratio $S^{2+}/S^+ = 4.5$ in this instance. Beyond 7 R_J the density decreases at a steeper rate, becoming lost in sky background noise beyond 7.5 R_J. The [SII] 6716/6731 doublet ratio, which is sensitive to n_e, increases with distance from Jupiter. Values of n_e, as computed from the doublet ratio, decrease at approximately the same rate as n_I. This indicates that the bulk ion population in the outer torus (including species and ionization states not observed in this work) has structure similar to the sulfur in the hot outer torus. Error limits for determining $n_e n_I$ are probably no larger than the uncertainties in the theoretical rate coefficients, believed to be accurate to within 10 percent (*8*), but it is worth noting that a number of critical coefficients have been revised by factors as large as 2 over the past few years. The

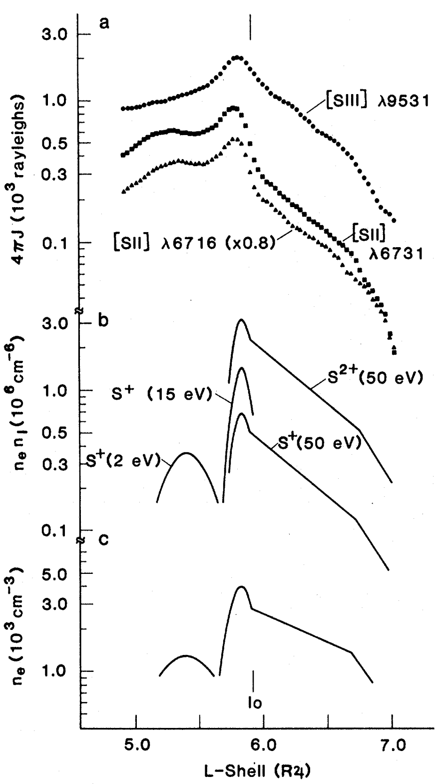

Fig. 2. Representative comparison of data and model for a set of three images taken on 4 May 1983, corresponding to the false-color image in Fig. 3b. (a) Curves showing a radial trace through the peak brightnesses in the image. The 6716-Å trace has been scaled for separation. (b) Curves showing the radial structure at the centrifugal equator in the three-dimensional torus components obtained by modeling the projected image brightnesses. The hot inner torus has been resolved into two distinct temperature components, as indicated. (c) Curve showing the radial structure in apparent electron density at the equator.

calculation of n_e from the [SII] doublet ratio is more sensitive to measurement errors; a 10 percent error propagates to a factor of about 30 percent in the inferred n_e. Hence density ratios, which give the radial and latitudinal scale heights, T_I, and ion partitioning, are more accurately determined than the absolute n_e values. Nevertheless, the resulting numbers indicate that sulfur comprises at least half the ion population in the hot outer torus.

Hot inner torus. The component of the hot torus residing inside Io's L-shell is characterized by a thin and sharply defined ribbon-like structure extending north-south along Jupiter's magnetic field lines. It is composed of an inward extension of the hot outer torus, with its common temperature (~50 eV) S^+ and S^{2+}, and the spatially close superposition of a generally cooler (7 to 35 eV) component composed predominantly of S^+. It is clear from the data that a continuum of temperatures is present in the hot inner torus. In the present work two model ion populations have been superimposed, the inward extension of the 50-eV population and an additional component at 15 eV. The cooler material found just inside Io's orbit appears to be isolated from that in the hot outer torus, with a distinct evolutionary history. The relative brightness between this cooler inner region and the common-temperature hot regions has been seen to vary by factors of 4 over the past three apparitions while maintaining the ribbon-like appearance seen in the present images.

The component with a temperature of 7 to 35 eV shows significant system III variations in both radial extent and T_I. In data spanning the 1981 to 1983 apparitions, S^+ ions are consistently hotter and are confined more closely (within ~0.05 R_J) to Io's orbit near $\ell_{III} = 200°$ and are consistently cooler and more inwardly extended (~0.2 R_J) on the opposite side near 20°. The radial extent evident in Fig. 2, about 0.2 R_J or four Io diameters, is among the largest widths seen in the 1983 data set. These tendencies indicate that the hot inner plasma is modified by longitudinal structure in Jupiter's magnetic field (*10*). On the basis of its apparent 360° period, the most likely cause is the Jovian dipole offset, which alters the magnetic field at Io's orbit as a function of system III longitude.

Approximating n_I just inside Io's orbit by a power law in radius, $n_I \alpha r^{-m}$, one finds $m > 10$. Since the plasma is confined by the Jovian dipole field and kept near the equator by centrifugal forces, radial diffusion of ions is driven by gradients in $(n_I r^3)$ (*11*). Hence the observed density gradient drives ion diffusion radially outward from 5.7 $R_{♃}$ through Io's orbit, precluding Io's orbit as the primary site for ionization of material found in the hot inner torus. The orbital motion of neutral material ejected from Io will populate the hot inner torus with atoms (*12*), which can be subsequently ionized predominantly in this inner region to form the "ribbon" structure.

Cool inner torus. The cool inner torus appears consistently between 5.3 and 5.6 $R_{♃}$ at the lowest T_I (2 to 3 eV) found in the nebula. The dominant sulfur ion is S^+ (S^{2+} is not observed in this inner region). The cool inner torus has appeared with roughly the same radial structure and temperatures in observations dating back to 1976, and it is thus the most permanent feature in the nebula. The cool torus was the predominant feature in the Jovian nebula in one well-documented case (*13*), with densities of hot inner and outer torus ions smaller by at least an order of magnitude than those present in post-Voyager images.

Discussion. The Jovian nebula contains a rich variety of observable characteristics, which are usefully organized in terms of three main toroidal components. Although it appears certain that sulfur and oxygen dominate the heavy ion population in the Jovian magnetosphere, the relative abundances remain uncertain and could very well be variable. A recent analysis of Voyager images of Io (*14*), indicates that two major types of volcanic resurfacing events determine the elemental composition available for sputtering by magnetospheric particles and ultimately the composition of magnetospheric ions. If the composition of newly sputtered material reaching the magnetosphere reflects the relative abundances on Io's surface, then sulfur would be the predominant ion, consistent with the results of the present work, and the ion abundance ratios of sulfur to oxygen could change in response to geological activity on Io. A recent analysis of ion composition and partitioning in the hot outer torus (*15*) indicates that a sulfur/oxygen ratio of 8 to 1 is optimum for consistency with a representative set of torus observations, whereas Voyager measurements in the outer magnetosphere favor sulfur over oxygen by a smaller margin (*1*). Future observations are likely to find the torus in the transient conditions that may follow a large geological event on Io or in an extended period of relative inactivity.

The importance of the radial diffusion of ions from Io due to flux-tube interchange has received considerable theoretical attention (*16*). Outward diffusion on time scales shorter than ion recombination times is an attractive mechanism in the present context, since it provides a natural explanation for the fixed S^{2+}/S^+ partitioning in the hot outer torus. However, outward diffusion of these ions would be accompanied by plasma cooling conserving the first two adiabatic invariants of ion motion in the Jovian magnetic field (*17*). If the outward diffusion takes place in time scales longer than the radiative cooling lifetime of the plasma ions, then the trend toward decreasing temperature with increasing radius would be strengthened. Consistent evidence for at most weak variations in T_I with radius in the hot outer torus, in both the present data and the Voyager 1 plasma science results (*6*), indicates that additional transport processes must be considered. By analogy with predictions for neutral oxygen (*12*) (which has its first ionization potential in the same range as sulfur), we expect that sputtered neutral sulfur in orbit near Io will produce a region of ionization showing a close similarity to the S^{2+} and S^+ distributions observed in the hot outer torus. The spatial distribution of neutral sulfur has not as yet been observed, although a spectroscopic detection has been reported (*18*).

A variety of energy-transfer mechanisms are active and important in the Jovian nebula. Charge exchange reactions must be important in the initial ionization of neutrals and in establishing the observed ion partitioning (*19*). The observed ~50-eV sulfur T_I values in the outer torus can be explained in terms of ion-electron Coulomb interactions between newly formed ions at pickup energies (~500 eV) and a background population of 5-eV electrons (*20*). Voyager 1 measurements indicate the presence of a small population (<1 percent) of electrons in the outer torus at 1-keV energies (*21*), which is important for ion partitioning (*15*). The relative importance of these competing processes must ultimately be tested by observation.

Earth-based imaging of the [SII] and [SIII] emissions from the Jovian nebula

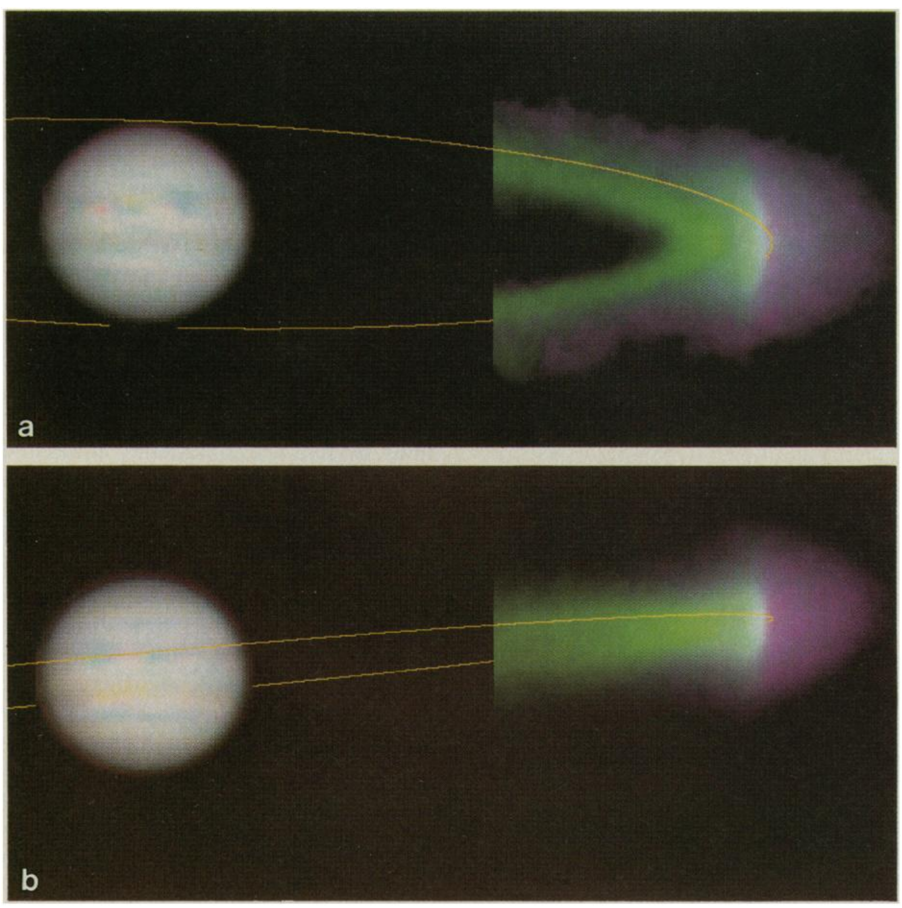

Fig. 3. The Jovian sulfur nebula, shown in false-color images which depict the nebula at two rotational phases (a and b) separated by 3 hours, obtained at Las Campanas Observatory on 4 May 1983. Regions populated predominantly in S^{2+} appear with purple hues, those predominantly S^+ appear green. The yellow curves mark the magnetic-centrifugal confinement equator associated with the orbital path of Io. Each image is a composite assembled from 0.1-second exposures of Jupiter for spatial reference, and subsequent 10-minute exposures of the nebula in characteristic [SIII] 9531-Å and [SII] 6731-Å emissions while blocking the Jovian disk.

confirms the presence of a plasma torus resembling in many respects the 1979 Voyager picture. These observations extend the Voyager snapshot in time, and a number of important regularities have been seen. Earth-based observations can bridge the gap between Voyager and future spacecraft measurements. The planned tour of the Jovian system by the Galileo spacecraft in 1989–1990 will provide a unique opportunity to carry out extensive ground-based measurements in conjunction with an Io flyby and a yearlong spacecraft presence in the nebula.

JOHN T. TRAUGER
Division of Geological and Planetary Sciences, California Institute of Technology, Pasadena 91125

References and Notes

1. See the Voyager 1 issue of *Science* [**204**, 945 (1979)].
2. M. H. Acuña, K. W. Behannon, J. E. P. Connerny, in *Physics of the Jovian Magnetosphere*, A. J. Dessler, Ed. (Cambridge Univ. Press, New York, 1983), p. 1.
3. T. W. Hill, A. J. Dessler, F. C. Michel, *Geophys. Res. Lett.* **1**, 3 (1974).
4. For recent reviews, see: C. B. Pilcher and D. F. Strobel, in *Satellites of Jupiter*, D. Morrison, Ed. (Univ. of Arizona Press, Tucson, 1982), p. 807; R. A. Brown, C. B. Pilcher, D. F. Strobel, in *Physics of the Jovian Magnetosphere*, A. J. Dessler, Ed. (Cambridge, Univ. Press, New York, 1983), p. 197.
5. D. E. Osterbrock, *Astrophysics of Gaseous Nebulae* (Freeman, San Francisco, 1974).
6. F. Bagenal and J. D. Sullivan, *J. Geophys. Res.* **86**, 8447 (1981).
7. T. W. Hill and F. C. Michel, *ibid.* **81**, 4561 (1976).
8. Rate coefficients have been calculated with the data collected by C. Mendoza, in *Planetary Nebulae, International Astronomical Union Symposium, No. 103*, D. R. Flower, Ed. (Reidel, Boston, 1983), p. 143.
9. B. R. Sandel *et al.*, *Science* **206**, 962 (1979).
10. T. W. Hill, A. J. Dessler, C. K. Goertz, in *Physics of the Jovian Magnetosphere*, A. J. Dessler, Ed. (Cambridge Univ. Press, New York, 1983), p. 353.
11. L. Froidevaux, *Geophys. Res. Lett.* **7**, 33 (1980).
12. W. H. Smyth and D. E. Shemansky, *Astrophys. J.* **271**, 865 (1983).
13. J. T. Trauger, G. Münch, F. L. Roesler, *ibid.* **236**, 1035 (1980).
14. A. S. McEwen and L. A. Soderblom, *Icarus* **55**, 191 (1983).
15. M. A. Moreno, W. I. Newman, M. G. Kivelson, unpublished data.
16. J. D. Richardson, G. L. Siscoe, F. Bagenal, J. D. Sullivan, *Geophys. Res. Lett.* **7**, 37 (1980).
17. G. L. Siscoe, *J. Geophys. Res.* **82**, 1641 (1977).
18. S. T. Durrance, P. D. Feldman, H. A. Weaver, *Astrophys. J.* **267**, 425 (1983).
19. R. E. Johnson and D. F. Strobel, *J. Geophys. Res.* **87**, 10385 (1982).
20. D. D. Barbosa, F. V. Coroniti, A. Eviatar, *Astrophys. J.* **274**, 429 (1983).
21. J. D. Scudder, E. C. Sittler, H. S. Bridge, *J. Geophys. Res.* **86**, 8157 (1981).
22. This work has been supported through NASA grant NAS 7-918 to the Jet Propulsion Laboratory.

16 April 1984; accepted 16 July 1984

Photocontraction of Liquid Spiropyran-Merocyanine Films

Abstract. *Amorphous films of a photochromic spiropyran containing a mesogenic group melt, when exposed to heat together with irradiation, to yield a red fluid. This fluid contains aggregates of merocyanine molecules and exhibits marked contraction under light illumination. The mechanism of the photocontraction is dependent upon a specialized microstructure, which may be termed a "quasi-liquid."*

The reversible transformation of spiropyrans, **1a**, into merocyanine dyes, **1b**,

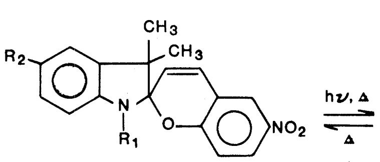

1a

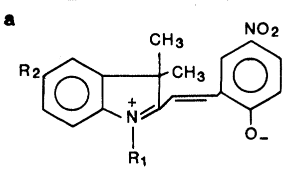

1b

determines the photo- and thermochromic properties of these compounds (*1*). This transformation is also responsible for the formation by these compounds of a variety of assemblies (*2–6*), based on the capability of the merocyanine dyes to give tightly bound giant molecular aggregates (*7*). These aggregates are molecular stacks of two types: H-aggregates, which exhibit an absorption that is blue-shifted relative to that of the nonaggregated dye, and J-aggregates, which exhibit a red-shifted absorption. The J- and H-aggregates have, respectively, parallel and antiparallel arrangements of the molecular dipoles in a stack.

One of the reported molecular assemblies is the "quasi-crystal" formed on photochromic conversion of spiropyrans into merocyanines in an electrostatic field. This consists of highly dipolar assemblies of molecular stacks of the J-type, covered by amorphous envelopes and forming submicron-sized globules aligned along the field (*2–4*). Polyvinyl macromolecules with spiropyran side groups give other types of assemblies with intra- and intermolecular stacking of merocyanine side groups in H-aggregates (*5, 6*).

Recently (*8*) we reported a new type of spiropyran-merocyanine assembly, termed quasi-liquid crystals, obtained from spiropyrans containing mesogenic groups (R_2 = –N=CHPhCOOPhX; X = $-OCH_3$, $-OC_6H_{13}$, –CN, where Ph is phenyl). These materials exhibit some features of conventional liquid crystals (birefringence and response to an electric field) but have completely different structure.

In a search for quasi-liquid crystals we synthesized spiropyran compounds **2** of the general formula **1a**, where R_1 = $-(CH_2)_6OOCPhOOCPhX$ and R_2 = –H. These T-shaped molecules, in contrast to the rod-like ones that form quasi-liquid crystals, do not exhibit mesophase properties. However, the melt of one of them, that with X = –CN, reveals a very unusual and intriguing photocontraction effect. This melt, produced by the irradiation and heating of amorphous films of the material, contracts markedly under irradiation.

The synthesis of spiropyrans **2** was from spiropyrans **1**, having R_1 = $-C_6H_{12}OH$ and R_2 = –H (*9, 10*), by direct esterification with acids XPhCOOPhCOOH (*11, 12*). The materials were purified by flash chromatography (*13*), the yields being about 60 percent. Yellow crystals of **2a** (X = –CN) and **2b** (X = $-OCH_3$) melt at 120° to 121°C and 118° to 119°C, respectively, to form fluids that are blue because of the presence of some merocyanine molecules formed spontaneously from the spiropyrans (*1*).

The amorphous films were obtained by fast evaporation of the solvent from a solution of the spiropyran in benzene on a glass surface, with subsequent removal of the residual solvent under vacuum. The grease-like films prepared in this way are metastable, and crystallization occurs after several hours (*8*).

The films were prepared between two cover glasses that were separated by spacers of aluminum foil and clamped together. For studies of the thermal behavior of the films, these "sandwiches" were placed on the hot stage of a polarizing microscope (Wild M8). When the films were heated at about 85°C, they were transformed to a fluid that was blue like the melts from the crystals.

Irradiation (nonfiltered light with an intensity of 10^{-6} to 10^{-7} einstein cm^{-1} sec^{-1} from an Osram HBO 200 mercury lamp) of the blue melt films of spiropyrans **2a** above 85°C produces red spots or stripes that disappear in the dark. However, if an amorphous film is irradiated during slow heating from room temperature to about 60° to 70°C, it acquires a uniform, stable, cherry-red color. This color does not disappear even at temperatures higher than 85°C. (In some cases several tiny spiropyran crystals appeared during preparation or storage of the amorphous films; irradiation led to the transformation of these crystals to